Zero-frequency spectral peaks of underdamped nonlinear oscillators with asymmetric potentials

M. I. Dykman

Institute of Semiconductors, Ukrainian Soviet Socialist Republic Academy of Sciences, Kiev, U.S.S.R.

R. Mannella* and P. V. E. McClintock

Department of Physics, University of Lancaster, Lancaster LA1 4YB, United Kingdom

S. M. Soskin

Institute of Semiconductors, Ukrainian Soviet Socialist Republic Academy of Sciences, Kiev, U.S.S.R.

N. G. Stocks

Department of Physics, University of Lancaster, Lancaster LA1 4YB, United Kingdom

(Received 10 September 1990)

The spectral density of the fluctuations of an underdamped, single-well, nonlinear oscillator driven by a random force has been investigated. Electronic analog experiments have demonstrated the existence of a narrow spectral peak at zero frequency; such a peak only appears, however, in those cases where the potential is non-centro-symmetric. The evolution of the peak with variation of a parameter characterizing the asymmetry of the potential, and with noise intensity, has been investigated both experimentally and theoretically. It is found that the half-width of the peak remains relatively small (of the order of the reciprocal relaxation time) over a broad range of noise intensities. The theory of the peak shape is shown to be in close agreement with experiment. The relationships of the peak to the (apparently similar) zero-frequency peaks observed previously in double-well oscillators, where they are responsible for stochastic resonance, and to the supernarrow spectral peaks found near kinetic phase transitions in periodically driven systems, are discussed.

I. INTRODUCTION

There are many physical systems that can be well described by nonlinear oscillators. The frequency spectrum of the conservative periodic eigenvibrations of such an oscillator for given energy E consists of the fundamental frequency $\omega(E)$ and, due to nonlinearity, a series of harmonics $n\omega(E)$ with $n = 2, 3, \ldots$. For an oscillator with a centrosymmetric potential, only the odd $(n = 3, 5, \ldots)$ harmonics are present. In the case of asymmetric potentials, on the other hand, the even $(n = 2, 4, \ldots)$ harmonics are present as well; furthermore, the equilibrium position $q_0(E)$ of the oscillator is dependent on energy.

Because of relaxation effects, and as a result of the fluctuations ubiquitous to real physical systems, the frequencies of the vibrations are in practice smeared. The fluctuational behavior of a vibrating system of this kind is best described in terms of the spectral density of its fluctuations, $Q(\Omega)$,

$$Q(\Omega) = \frac{1}{\pi} \mathrm{Re} \int_0^\infty dt \, \langle [q(t) - \langle q \rangle][q(0) - \langle q \rangle] \rangle e^{i\Omega t} \, , \quad (1)$$

where q is the coordinate of the system and $\langle \cdots \rangle$ denotes ensemble averaging. For thermal equilibrium systems the function $Q(\Omega)$ determines the susceptibility, including the absorption coefficient.[1] In the case of underdamped oscillators with relatively weak nonlinearity, the function $Q(\Omega)$ has peaks near the fundamental frequency $\omega(0)$ of small amplitude vibrations about the equilibrium position and its overtones (the energy E being

measured from the bottom of the potential well). These peaks correspond to the Fourier components of the eigenoscillations mentioned above.

It was shown in Ref. 2 that, in addition to the spectral peaks at finite (nonzero) frequency, a peak also arises at zero frequency in the case of oscillators with asymmetric potentials. The zero-frequency peak can be considered as a "continuation" downwards of the even harmonic series $(n = 2, 4, \ldots)$ to $n = 0$. It is due simply to the dependence of the equilibrium position $q_0(E)$ of the oscillator on its energy. It is precisely this dependence that gives rise to the fluctuations of $q_0(E)$ which accompany the fluctuations of the energy E. The former do not have any characteristic frequency and are relatively slow, so that they give rise to a spectral peak at zero frequency. Their characteristic time scale is given by the reciprocal damping constant Γ^{-1}, which substantially exceeds the characteristic period of the vibrations $2\pi\omega^{-1}(0)$. Consequently, the width of the zero-frequency peak, $\sim \Gamma$, is small compared to $\omega(0)$. A corresponding peak in the absorption spectra of weakly nonlinear localized vibrations in solids was predicted on the basis of quantum theory by Krivoglaz and Pinkevich.[3]

We note that, for underdamped systems of the kind under consideration, the zero-frequency peaks arise *in addition* to the peaks near eigenfrequencies and their overtones. For overdamped (or very strongly damped) systems, on the other hand, no matter whether they are linear[1,4] or nonlinear,[5] relatively broad zero-frequency peaks are the only maxima in the spectral densities of

their fluctuations.

A zero-frequency peak in $Q(\Omega)$ for an underdamped oscillator with a double-well potential has been observed both in electronic experiments[2] and numerical calculations[6] and was investigated analytically in Ref. 2. However, in the such potentials there are *two* mechanisms contributing to the peak: the mechanism described above; and a second one associated with the noise-induced interwell transitions[7] (cf. also Ref. 8 where the case of overdamped motion was considered). In the present case, for an underdamped oscillator with a single-well potential, the latter mechanism clearly cannot occur and we are thus able to study in isolation the zero-frequency peak arising purely from the slow variations of $q_0(E)$.

In the present paper, the zero-frequency peak is investigated by means of an analog electronic experiment, and described theoretically, for the single-well, underdamped, nonlinear oscillator already analyzed in Ref. 9 (hereinafter referred to as I): it corresponds to a Brownian particle vibrating in a potential with a quartic nonlinearity and a superimposed homogeneous field. The equation of motion is of the form

$$\ddot{q}+2\Gamma\dot{q}+\frac{\partial U}{\partial q}=f(t) \ ,$$
$$U(q)=\tfrac{1}{2}q^2+\tfrac{1}{4}q^4+Aq \ , \qquad (2)$$
$$\langle f(t)f(t')\rangle=4\Gamma T\delta(t-t') \ .$$

Here, $f(t)$ is white Gaussian noise of characteristic intensity T; when both the friction and the noise originate from coupling of the oscillator to a thermal bath, T is equal to the temperature of the latter. The term Aq in the potential $U(q)$ represents the homogeneous field acting upon the oscillator; it is this term that removes the inversion symmetry of the potential $U(q)$ and is thus responsible for the appearance of the zero-frequency peak. As already mentioned in I, the model (2) refers to a number of physical systems, and in particular to localized vibrations in solids,[10] where the "strength of the homogeneous field" A can readily be varied.

The theory of the zero-frequency peak for an underdamped oscillator is developed in Sec. II. Experimental results obtained from an electronic model of (2) are presented in Sec. III. In Sec. IV, the theory of Sec. II is applied to the model (2) and the theoretical and experimental results are compared with each other. Section V contains concluding remarks.

II. THEORY OF THE ZERO-FREQUENCY PEAK

The main factors that determine the shape of the spectral density of the fluctuations (1) of a single-well nonlinear oscillator (cf. Ref. 7) are (i) the presence of the overtones of the vibrations of a given energy; (ii) straggling of the vibrational eigenfrequency $\omega(E)$ due to energy straggling [that is, to the finite width ($\sim T$) of the oscillator's energy distribution]; and (iii) smearing of the eigenfrequency $\omega(E)$ due to relaxation of the oscillator. (Some other relevant factors are discussed in Ref. 11; see

also I.)

We shall consider underdamped oscillators whose damping is small compared to their eigenfrequencies,

$$\Gamma \ll \omega(E) \ , \qquad (3)$$

for the case of energies $E \lesssim T$. Here, and in what follows, we take the zero of potential energy to be its value $U(q_{eq})$ in the equilibrium position q_{eq}, for which $U'(q_{eq})=0$.

Where the intensity T of the external noise is not too high so that, in addition to the inequality (3), the frequency straggling is also small,

$$\delta\omega \ll \omega(0), \quad \delta\omega=\max|\omega(E)-\omega(0)| \qquad (4)$$

for $E \lesssim T$, the peaks in $Q(\Omega)$ corresponding to the overtones of the eigenvibrations do not overlap. The shapes of the peaks are determined by the two broadening mechanisms mentioned above, namely, the frequency straggling and the relaxational smearing of the eigenfrequency. For sufficiently strong noise intensities, when $\delta\omega \gg \Gamma$, the first of those mechanisms must obviously be dominant, so that the characteristic widths of the peaks then substantially exceed the relaxational broadening. A detailed experimental and theoretical investigation of the peak of $Q(\Omega)$ at the fundamental frequency for the model (2) has already been presented in I.

It is evident that frequency straggling should not influence the shape of the zero-frequency peak directly: this is because the latter is connected, not with the periodic vibrations of the coordinate as such, but with the (slow) fluctuations of its mean value $q_0(E)$. Thus the zero-frequency peak is expected to be much narrower than the other peaks in $Q(\Omega)$, for not too small noise intensities, such that $\delta\omega \gg \Gamma$. Moreover, it would be well resolved, irrespective of the ratio $\delta\omega/\omega(0)$, provided that (3) is fulfilled.

A convenient approach to the calculation of the spectral density of the fluctuations is based[7,12] on the appropriate Fokker-Planck equation. An analysis of the properly transformed Fokker-Planck equation (see I) subject to the condition (3) shows that $Q(\Omega)$ in the region of its peaks is formed, to lowest order in $\Gamma/\omega(E)$, from a superposition of the peaks themselves with a smooth background. The shape of the peak at the nth overtone is described by the spectral density of fluctuations of the nth harmonic $q_n(E)$ of the coordinate. The latter is determined from the equations of the conservative motion,

$$\omega(E)\frac{\partial q(E,\phi)}{\partial\phi}=p(E,\phi) \ ,$$
$$\omega(E)\frac{\partial p(E,\phi)}{\partial\phi}=-\frac{\partial U(q)}{\partial q} \ ,$$
$$E=\tfrac{1}{2}p^2+U(q)-U(q_{eq}) \ , \qquad (5)$$
$$U'(q_{eq})=0$$

(where p is the momentum of the oscillator and ϕ is its phase) as the Fourier component of the coordinate $q(E,\phi)$ over ϕ,

$$q_n(E)=\frac{1}{2\pi}\int_0^{2\pi}d\phi \exp(-in\phi)q(E,\phi) \ . \qquad (6)$$

This is also the case for the zero-frequency peak. In the range of low frequencies

$$Q(\Omega) \simeq Q_b + Q_0(\Omega), \quad \Omega \ll \omega(E) , \quad (7)$$

where Q_b is the frequency-independent background caused by the harmonics $q_n(E)$ with $n \neq 0$ [the relaxation-induced "tail" of the peak of $Q(\Omega)$ due to the eigenoscillations], and $Q_0(\Omega)$ describes the shape of the zero-frequency peak and is given by the spectral density of the fluctuations of the "smooth" component of the coordinate q_0,

$$Q_0(\Omega) = \frac{1}{\pi} \text{Re} \int_0^\infty dt \langle \{q_0[E(t)] - \langle q \rangle\}$$
$$\times \{q_0[E(0)] - \langle q \rangle\} \rangle \exp(i\Omega t) . \quad (8)$$

By making use of the results of I based on the Fokker-Planck equation, the function $Q_0(\Omega)$ can be written as

$$Q_0(\Omega) = \text{Re} \int_0^\infty dE \, \omega^{-1}(E) q_0(E) W_0(E,\Omega) , \quad (9)$$

where $W_0(E,\Omega)$ is the Fourier transform over time of the zeroth harmonic (in ϕ) of the probability density (integrated over initial conditions with the proper weight) for the oscillator performing Brownian motion. It satisfies the equation

$$i\Omega W_0 + 2\Gamma \omega(E) \frac{\partial}{\partial E} \left[\omega^{-1}(E) \overline{p^2} \left[1 + T \frac{\partial}{\partial E} \right] W_0 \right]$$
$$= -2[q_0(E) - \langle q \rangle] w_{st}(E), \quad (10)$$

$$\overline{p^2} \equiv \overline{p^2(E)} = \frac{1}{2\pi} \int_0^{2\pi} d\phi \, p^2(E,\phi) ,$$

where $w_{st}(E)$ is the stationary distribution of the oscillator

$$w_{st}(E) = Z^{-1} \exp(-E/T) ,$$
$$Z = 2\pi \int_0^\infty dE \, \omega^{-1}(E) \exp(-E/T) . \quad (11)$$

Equation (10) is a second-order ordinary differential equation: note that the differential operator in the second term coincides with the operator describing the drift and diffusion of an underdamped system over energy, originally derived by Kramers.[13]

The boundary conditions for (10) follow from the physical meaning of $W_0(E,\Omega)$ as a component of the probability density. The first of them follows from the vanishing of the probability density for infinite energies,

$$W_0(E,\Omega) \to 0, \quad \text{for} E \to \infty . \quad (12a)$$

The second follows from the vanishing as $E \to \infty$ of the flow of the probability density along the energy axis, which (cf. Ref. 13) is proportional to $\omega^{-1}(E) \overline{p^2} (1 + T\partial/\partial E) W_0$. Integrating (10) over E with the weight $\omega^{-1}(E)$ and taking into account this property and the relation

$$\langle q \rangle = 2\pi \int dE \, \omega^{-1}(E) q_0(E) w_{st}(E) ,$$

we obtain

$$\int_0^\infty dE \, \omega^{-1}(E) W_0(E,\Omega) = 0 . \quad (12b)$$

The boundary condition (12b) is of the form of the integral equation. For a weakly nonlinear oscillator [$\omega(E) \simeq$ const] with a nonlinear friction force, such a condition was obtained in Ref. 12.

The boundary problem (10–12) can be solved numerically for an arbitrary potential. The simplest method is to find two solutions, $W_0^{(1)}$ and $W_0^{(2)}$ of (10) satisfying (12a) with some differing arbitrary $W_0^{(1)}(0,\Omega)$ and $W_0^{(2)}(0,\Omega)$. The solution is given by a linear combination

$$\alpha W_0^{(1)}(E,\Omega) + (1-\alpha) W_0^{(2)}(E,\Omega) ,$$

with the coefficient α chosen so that condition (12b) is satisfied. Numerical results obtained for the model (2) by this procedure are discussed in Sec. IV.

An analytic expression for $Q_0(\Omega)$ can be obtained for the case of comparatively weak noise. In deriving it we note that, for small energies, the quantities $q_0(E), \omega(E)$ can be series expanded as

$$q_0(E) = \mu_1 \left[\frac{E}{E_c} \right] + \mu_2 \left[\frac{E}{E_c} \right]^2 + \cdots ,$$

$$\omega(E) = \omega(0) \left[1 + \nu \left[\frac{E}{E_c} \right] + \cdots \right] . \quad (13)$$

We have chosen the origin of coordinates such that $q_0(0) = 0$; the quantity E_c gives a characteristic energy scale for the nonlinearity of the oscillator. To find the expression for $Q_0(\Omega)$ for noise intensities in the range $T \ll E_c$, it is convenient to transform from the differential equation (10) to the set of equations for the moments

$$M_n = \int_0^\infty dE \, \omega^{-1}(E) E^n W_0(E,\Omega) .$$

Decoupling this set at $n=2$ and allowing for the relation (cf. Ref. 4)

$$\frac{d[\omega^{-1}(E) \overline{p^2}]}{dE} = \omega^{-1}(E) ,$$

we obtain

$$Q_0(\Omega) \simeq \frac{1}{\pi} \mu_1^2 \left[\frac{T}{E_c} \right]^2 \frac{2\Gamma}{4\Gamma^2 + \Omega^2}$$
$$\times \left[1 + \frac{8T}{E_c} \left[\frac{\mu_2}{\mu_1} - \frac{2\nu\Gamma^2}{4\Gamma^2 + \Omega^2} \right] \right], \quad T \ll E_c .$$
$$(14)$$

It is evident from (14) that, to lowest order in T/E_c, the zero-frequency peak is described by a Lorentzian distribution centered on $\Omega = 0$ with a half-width $\delta\Omega = 2\Gamma$ (cf. Ref. 2). The intensity of the peak is proportional to $(T/E_c)^2$. The corrections $\sim T/E_c$ alter both the intensity and the shape of the peak. The latter is directly related to the frequency dispersion $(d\omega/dE \neq 0)$. It follows from (14) that the half-width of the peak,

$$\delta\Omega \simeq 2\Gamma(1+2\nu T/E_c) \; , \tag{15}$$

so, for $\nu \propto (d\omega/dE)_{E=0} > 0$, $\delta\Omega$ increases with increasing noise intensity T whereas, for $\nu < 0$, it decreases (it still being assumed that T/E_c is small). The results (14) and (15) are applied to the model (2) and compared with the experimental data in Sec. IV.

It is evident from (14) that the intensity of the zero-frequency peak decreases rapidly with decreasing T. For sufficiently small T/E_c, the main contribution to the low-frequency spectral density of fluctuations comes from the smooth background. To lowest order in T/E_c, this background [the Q_b term in Eq. (7)] is simply the relaxational part of the spectral density of fluctuations of the small amplitude (and thus almost harmonic) vibrations about the equilibrium position,

$$Q_b \simeq 2\Gamma T/\pi\omega^4(0), \quad T \ll E_c \; . \tag{16}$$

It is clear from (14) and (16) that the zero-frequency peak should become pronounced for noise intensities

$$T/E_c \gg [\Gamma/\omega(0)]^2[E_c/\mu_1^2\omega^2(0)] \; .$$

For underdamped non-centro-symmetric systems, where $\Gamma \ll \omega(0)$ and $E_c \sim \mu_1^2\omega^2(0)$, these intensities are quite small.

III. THE ANALOG ELECTRONIC EXPERIMENT

The analog electronic circuit used to model (2) in the present work was identical to that already described in connection with the experiments on noise-induced spectral narrowing in I. The experimentally determined value of the dimensionless damping coefficient was $\Gamma = 0.0143 \pm 0.0005$. Since the field parameter A could be varied easily, it was possible to confirm directly in the course of the experiments the absence of the zero-frequency peak for $A = 0$ when the potential of the oscil-
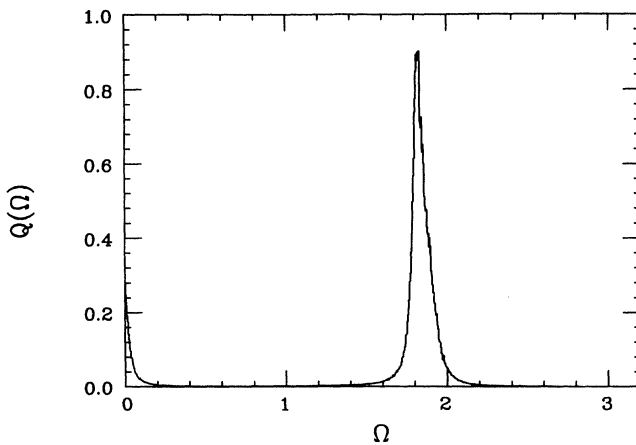

FIG. 1. Power spectral density $Q(\Omega)$ of the fluctuations measured for the electronic model of (2) with $A=2.0$, $T=0.814$. The full spectrum (except for the overtones) is plotted, with the zero-frequency peak on the left-hand side and the peak corresponding to eigenoscillations at the fundamental frequency on the right-hand side.
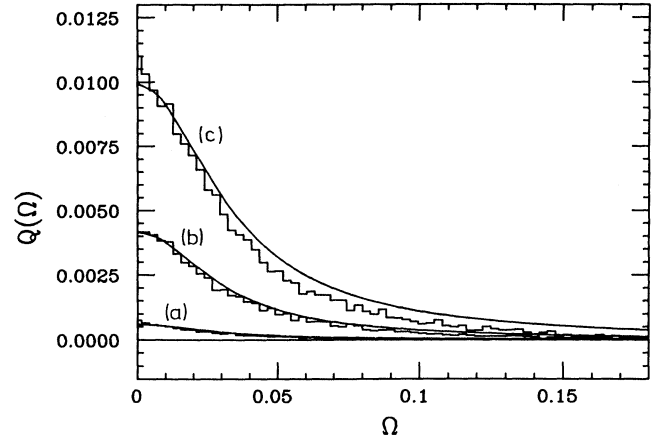

FIG. 2. The zero-frequency peak measured (histogram) and calculated (solid lines) for (2) with the field-strength parameter $A=0.2$ and noise intensities: (a) $T=0.0194$; (b) $T=0.0754$; (c) $T=0.222$.

lator is centrosymmetric, and the onset of the peak for finite A. The dependence on A of the shape and intensity of the peak could be investigated readily.

A typical power spectrum as measured for the circuit model is shown over its full frequency range by the histogram in Fig. 1 for the particular values $A=2$, $T=0.814$. In addition to the usual resonant maximum centered on a finite frequency, the expected peak at zero frequency is clearly resolved. Our main interest in the present paper relates, of course, to the zero-frequency peak itself, the (interesting) behavior of the resonant peak having already been discussed in detail in I. In what follows we will therefore concentrate our attention exclusively on the power spectrum at low frequencies; it must be borne in mind that the spectra as measured all necessarily include the resonant peak as well, even though it is not included in the other figures.

The existence of the resonant peak (and its overtones) gave rise to some experimental difficulties, in particular
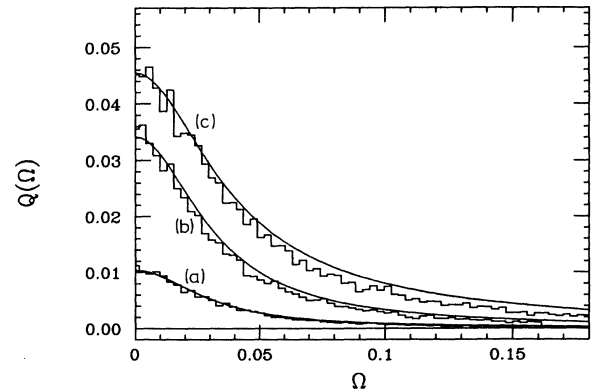

FIG. 3. The zero-frequency peak measured (histogram) and calculated (solid lines) for (2) with the field-strength parameter $A=0.43$ and (a) $T=0.0755$; (b) $T=0.223$; (c) $T=0.668$.
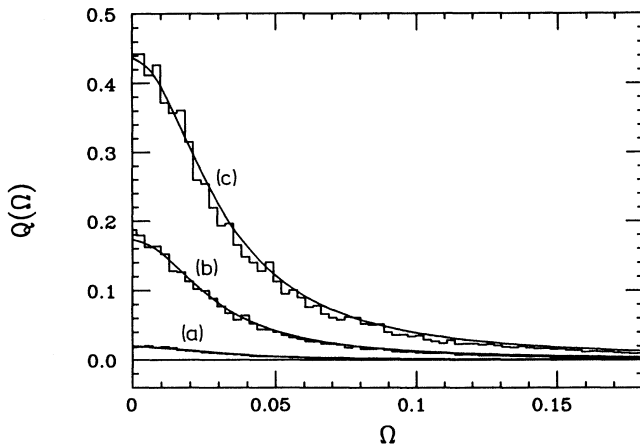
FIG. 4. The zero-frequency peak measured (histogram) and calculated (solid lines) for (2) with the field-strength parameter $A=2$ and noise intensities: (a) $T=0.222$; (b) $T=0.671$; (c) $T=1.58$.

FIG. 6. The half-width at half maximum (HWHM) $\delta\Omega$ of the zero-frequency peak plotted as a function of the noise intensity T for three values of the field-strength parameter: (a) $A=0.2$; (b) $A=0.43$; (c) $A=2.0$. The data points represent measurements on the electronic analog model; the solid curves represent the theory.

because it was often very much larger than the zero-frequency peak. There were two aspects to the problem. First, because the motion of the system was predominantly at frequencies close to the eigenfrequency $\omega(0)$, extremely long averaging periods were required to obtain acceptable statistical quality in the range of the zero-frequency peak. Second, the relatively very large amplitude of the resonant peak meant that the discrete fast Fourier transform (FFT) algorithm tended to "fold back" the high-frequency wing of the peak lying beyond the Nyquist frequency, thereby distorting the low plateau region of the spectrum between the two maxima. These problems were overcome by filtering the fluctuating voltage from the circuit with a single-pole filter whose time con-
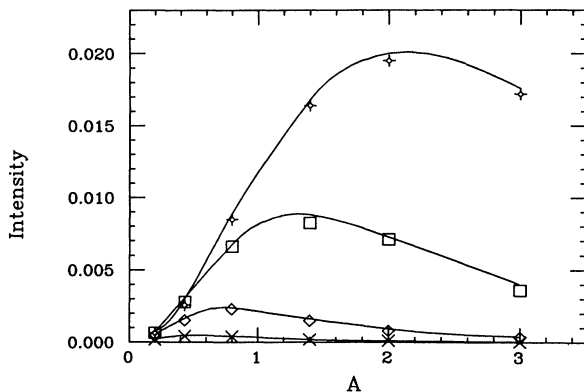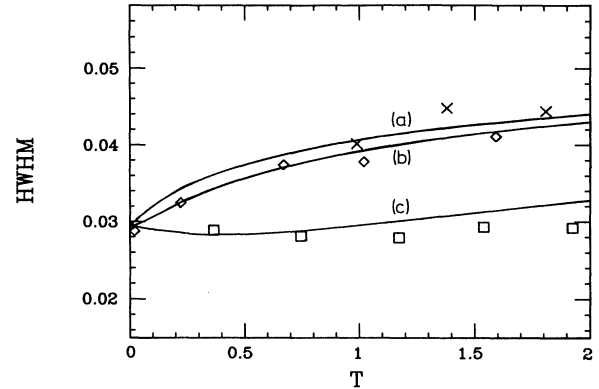
stant was chosen such that it drastically attenuated the resonant peak: its value was selected so as to reduce the spectral density by a factor of 300 at $\Omega=\omega(0)$. The effect on the zero-frequency peak, while very much smaller, was nonetheless to introduce significant distortion, and it was consequently necessary to divide the spectrum by an appropriate (frequency-dependent) compensating function. The latter was determined by measuring the power spectral density of quasiwhite noise that had been passed through the *same* filter. The procedure was tested by comparing the resonant peaks of the unfiltered, and the filtered/compensated, spectra measured under otherwise identical conditions, and was found to work well. It virtually eliminated problems associated with artifacts arising from the "folding back" of frequencies beyond the Nyquist frequency.

When the circuit was adjusted so as to set $A=0$, (i.e., a centrosymmetric potential), no peak was seen at zero frequency; the peak appeared *only* for finite A. The evolution of the peak with varying values of A and T is shown by the histograms in Figs. 2–4. The peak is well resolved and can be separated easily from the smooth background for the parameter ranges in question.

The variation of the intensity (integrated area) of the zero-frequency peak with A is shown for several values of T by the data points in Fig. 5. The measured half-width at half maximum (HWHM) $\delta\Omega$ is shown as a function of T for three values of A by the points in Fig. 6.

FIG. 5. The integrated intensity of the zero-frequency peak (with the background subtracted) plotted as a function of the field-strength parameter A. The data points represent measurements on the electronic analog model of (2); the solid curves represent the theory. The noise intensities for the five curves and associated data, reading from bottom to top, were $T=0.0754$, 0.222, 0.671, and 1.58.

IV. DISCUSSION OF RESULTS

The low-frequency spectra $Q(\Omega)$ measured experimentally (histograms) are compared with those calculated numerically (solid curves) from (9)–(12) in Figs. 2–4. To obtain the coefficients $\omega(E), p^2(E), q_0(E)$ in these equations, the results of I were used. The spectral background Q_b in (7) was not, however, computed. Rather, in the comparison of experiment and theory, a small vertical

adjustment was made in the latter; this procedure did not affect significantly the comparison of the calculated and measured peak shapes or intensities. Apart from this, there were no other adjustable parameters; the experimental and theoretical scales of $Q(\Omega)$ and Ω, and the values of Γ, A, and T in (2) were all absolute. It is evident from Figs. 2–4 that the theory fits the experimental data well, both qualitatively and quantitatively.

A peculiar feature of the system (2) is the nonmonotonic dependence of the intensity I of the zero-frequency peak (where we mean the intensity of the whole "zero-frequency" peak, including the part at negative frequencies, which is symmetric to that at positive frequencies) on the "field" A (see Fig. 5). It is also immediately apparent that the dependence of its half-width $\delta\Omega$ on the noise intensity T can take quite different forms, depending on the value of A (see Fig. 6). For small T, both of these features follow from (14) and (15) if one takes account of the explicit form of the coefficients μ_1, v in (13) for the particular case of (2). These coefficients can be obtained readily either by direct analysis of (2) or, more conveniently, by making use of the results given in I:

$$\frac{\mu_1}{E_c} = \frac{3q_{eq}}{(1+3q_{eq}^2)^2} , \quad \frac{v}{E_c} = \frac{3}{4}\frac{1-7q_{eq}^2}{(1+3q_{eq}^2)^3} . \tag{17}$$

Here, q_{eq} is the equilibrium position of the oscillator. It is evident from (2) that it is given by the solution of

$$q_{eq}^3 + q_{eq} + A = 0 . \tag{18}$$

The characteristic energy E_c for the oscillator (2) is $(1+3q_{eq}^2)^2$; cf. (17).

According to (14) and (17), the intensity I of the zero-frequency peak

$$I = \int_{-\infty}^{\infty} d\Omega \, Q(\Omega) = \langle q_0^2(E) \rangle - \langle q_0(E) \rangle^2 \tag{19}$$

is proportional to $q_{eq}^2/(1+3q_{eq}^2)^4$ for small T/E_c. Therefore, taking account of (18), $I \propto A^2$ for $|A| \ll 1$. [Of course $I=0$ for $A=0$ because it is the term Aq in the potential $U(q)$ in (2) that makes $U(q)$ non-centro-symmetric.] For $|A| \gg 1$, on the other hand, $I \propto |A|^{-2}$. Thus I at first increases with increasing $|A|$, and then decreases again. The maximum of I occurs for $|A| = \frac{10}{27}$ if $T/E_c \ll 1$. A qualitative explanation for the decrease of I for large $|A|$ can be found in terms of the suppression of fluctuations due to the increasing "rigidity" of the system in this range of A [$\omega(0) \propto |A|^{1/3}$, $E_c \propto |A|^{4/3}$ for $|A| \gg 1$]. Thus the nonmonotonicity of $I(A)$ is expected to occur irrespective of temperature. This is confirmed both by the calculations based on (19) and by the experiment, as shown in Fig. 5. The position of the maximum in I shifts to higher $|A|$ with increasing T; and I itself also increases with increasing T: cf. (14).

To account for the behavior of the half-width $\delta\Omega$ of the zero-frequency peak (see Fig. 6), we could emphasize once again that this peak is due to the fluctuations and relaxation of the oscillator energy E. The relaxation of its energy $\bar{E}$ averaged over the vibrational period and over realizations of the random force is described by the well-known equation
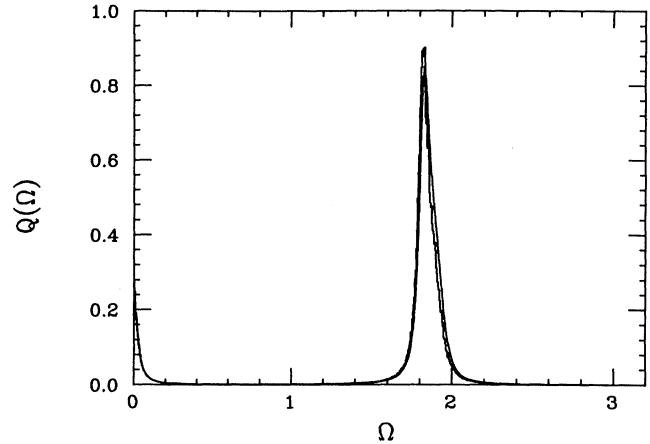
$$\frac{d\bar{E}}{dt} = -2\Gamma\overline{p^2(\bar{E})} + 2\Gamma T . \tag{20}$$

The "differential friction coefficient" determining the energy relaxation is

$$2\Gamma\overline{dp^2}/d\bar{E} = 2\Gamma\{1 + \overline{p^2}d[\ln\omega(\bar{E})]/d\bar{E}\} .$$

For $d\omega(E)/dE > 0$, this coefficient exceeds 2Γ. It is natural, therefore, that the half-width of the peak of $Q_0(\Omega)$, which is determined just by the energy relaxation time, should exceed 2Γ in this case. It increases with T for $T \lesssim E_c$, since $q_0(E)$ increases with E for $E \lesssim E_c$ and therefore the actual energies are $E \sim T$. For the opposite case of negative $d\omega(E)/dE$, on the other hand, the half-width should decrease with T for $T < E_c$. These qualitative arguments are confirmed in the low T/E_c limit by the explicit expression (15). It should be noted that the half-width of the zero-frequency peak for $T \gg \Gamma/|d\omega(E)/dE|_{E=0}$ [an inequality that is compatible with $T \ll E_c$ for $\Gamma \ll \omega(E)$] is much smaller than those of the peaks at the fundamental frequency and overtones, which are determined by frequency straggling in this range of temperatures (cf. Ref. 7). The agreement between experiment (data points) and theory (full curves) in Fig. 6 may be regarded as satisfactory: the fit for $A=0.2$ is the least good; but, given that the zero-frequency peak was then smaller than the resonant peak by more than two orders of magnitude, the quality of the agreement is in fact remarkable.

Taken in conjunction with the theory of the peak at the fundamental frequency given in I, the above discussion provides a good description of the spectral density over a wide range of frequencies. As an example, the power spectrum of Fig. 1 (histogram) is compared with theory (solid curve) in Fig. 7.

V. CONCLUSION

It follows from the above results that, in the spectra of non-centro-symmetric underdamped single-well oscilla-

tors, there arise well-resolved peaks at zero frequency. The width of the zero-frequency peak is close to the reciprocal relaxation time for the energy, and it varies smoothly with noise intensity. The intensity of the peak depends strongly upon the potential asymmetry; it vanishes in the case of a symmetric potential. In the particular model (2) investigated, an oscillator with fourth-order nonlinearity with asymmetry due to a homogeneous field, the intensity as a function of field strength is "domelike" in form.

We note that, although the zero-frequency peak may be thought of as one of the series of peaks at the overtones $n\omega(E)$ of a nonlinear oscillator, appearing at $n=0$, it is often much more prominent than the peaks at the other overtones ($n=2,3,\ldots$). This can be understood in the following way. The peaks at the overtones arise because of nonlinearity; the latter increases with the vibrational energy (at least for relatively small E) and hence the intensities of the peaks also increase with increasing noise intensity T (at least for $T \lesssim E_c$); but with increasing T, the width of the energy distribution and, correspondingly, the size of the frequency straggling, increase as well. Consequently, for rather small T, $E_c \gg T \gg \Gamma / |d\omega(E)/dE|_{E=0}$, the broadening of all peaks except the zero-frequency peak turns out to exceed substantially the relaxational broadening Γ. Thus the zero-frequency peak is much sharper and, correspondingly, more clearly resolved. At small T, $T \lesssim \Gamma / |d\omega(E)/dE|_{E=0} \ll E_c$, the widths of the zero-frequency and the second overtone ($n=2$) peaks are of the same order of magnitude and their intensities are of the same order in T [$\sim (T/E_c)^2$; the intensities of the peaks of $n > 2$ are $\sim (T/E_c)^n \ll (T/E_c)^2$]. However, the intensity of the peak at $\simeq 2\omega(0)$ is smaller by a factor of 9 than that of the zero-frequency peak: this can be demonstrated theoretically by making allowance for the lowest-order (cubic) nonlinearity of the oscillator potential which is significant at low energies and which is responsible for the peaks in question (cf. Ref. 14).

We note in conclusion that the onset of the zero-frequency peak discussed in this paper is one of the factors that complicate observations of stochastic reso-

nance[15-19] for double-well underdamped systems. This phenomenon is characterized by a domelike ("resonant") dependence of the signal-to-noise ratio (SNR) on the external noise intensity in periodically driven systems. The terms "signal" and "noise" are to be understood here in terms of the power spectrum, being defined, respectively, as the intensity of the spike at the field frequency, and the spectral density of the noisy background at the same frequency in the absence of the periodic force. The external-noise-induced increase of the SNR is due to the stimulation, by noise, of interwell transitions. It can be seen from Fig. 5 that, for the (single-well) oscillator studied in the present paper, $Q_0(\Omega)$ rises rapidly with increasing T: as already mentioned, this behavior is inherent to underdamped systems with non-centro-symmetric potentials. Exactly the same effect will be associated with vibrations within each of the individual (asymmetric) potential wells of the underdamped double-well oscillators for which stochastic resonance has been investigated. It results directly in an increase of the "noisy" denominator of the SNR. The corresponding reduction in the magnitude of the stochastic resonance effect can be larger than that associated with the relatively slow growth of the background Q_b in (7) with increasing noise intensity (the latter effect being common to both underdamped and overdamped systems). A detailed analysis of the SNR for weak periodic forcing can be accomplished[20] in terms of linear-response theory and will be presented in full elsewhere.[21]

ACKNOWLEDGMENTS

*Present address: Dipartimento di Fisica, Universita degli Studi di Pisa, Piazza Torricelli 2, 56100 Pisa, Italy.

[1]L. D. Landau and E. M. Lifshitz, *Statistical Physics*, 3rd ed. (Pergamon, New York, 1980), Part 1.

[2]M. I. Dykman, R. Mannella, P. V. E. McClintock, F. Moss, and S. M. Soskin, Phys. Rev. A **37**, 1303 (1988).

[3]M. A. Krivoglaz and I. P. Pinkevich, Zh. Eksp. Teor. Fiz. **51**, 1151 (1966) [Sov. Phys.—JETP **24**, 772 (1967)].

[4]L. D. Landau and E. M. Lifshitz, *Mechanics* (Pergamon, London, 1976).

[5]S. H. Crandall, in *Random Vibrations*, edited by S. H. Crandall (MIT Press, Cambridge, MA, 1963), Vol. 2, p. 85; J. B. Morton and S. Corrsin, J. Stat. Phys. **2**, 153 (1970); R. F. Rodriguez and N. G. van Kampen, Physica A **85**, 347 (1976); A. R. Bulsara, K. Lindenberg, and K. E. Shuler, J. Stat. Phys. **27**, 787 (1982).

[6]K. Voightlaender and H. Risken, J. Stat. Phys. **40**, 397 (1985).

[7]M. I. Dykman and M. A. Krivoglaz, in *Soviet Physics Reviews*, edited by I. M. Khalatnikov (Harwood Academic, New York, 1984), Vol. 5, p. 265.

[8]P. Hanggi and N. Thomas, Phys. Rep. **88**, 207 (1982).

[9]M. I. Dykman, R. Mannella, P. V. E. McClintock, S. M. Soskin, and N. G. Stocks, Phys. Rev. A **42**, 7041 (1990) referred to in text as I.

[10]A. S. Barker, Jr. and A. J. Sievers, Rev. Mod. Phys. **47**, Suppl. No. 2, S1 (1975).

[11]S. M. Soskin, Physica A **155**, 401 (1989).

[12]M. I. Dykman and M. A. Krivoglaz, Phys. Status Solidi B **68**, 111 (1975).

[13]H. A. Kramers, Physica (Utrecht) **7**, 284 (1940).

[14]M. I. Dykman and M. A. Krivoglaz, Ukr. Fiz. Zh. **17**, 1971 (1972).

[15]C. Nicolis, Tellus **34**, 1 (1982); R. Benzi, A. Sutera, and A. Vulpiani, *ibid*. **34**, 10 (1982).

[16]P. Jung and P. Hanggi, Europhys. Lett. **8**, 505 (1989).

[17]R. F. Fox, Phys. Rev. A **39**, 4148 (1989).

[18]G. Debnath, T. Zhou, and F. Moss, Phys. Rev. A **39**, 4323 (1989).

[19]B. McNamara and K. Wiesenfield, Phys. Rev. A **39**, 4854

(1989).

[20]M. I. Dykman, R. Mannella, P. V. E. McClintock, and N. G. Stocks, Pis'ma Zh. Eksp. Teor. Fiz. **52**, 780 (1990) [JETP Lett. (to be published)]; Phys. Rev. Lett. **65**, 2606 (1990).

[21]M. I. Dykman, R. Mannella, P. V. E. McClintock, and N. G. Stocks (unpublished).